ARMY RESEARCH LABORATORY

Characterization of Solution Synthesis of Zinc Complexes With Iron

by Amirh Whitt and James M. Sands

ARL-TN-309 **April 2008**

NOTICES

Disclaimers

The findings in this report are not to be construed as an official Department of the Army position unless so designated by other authorized documents.

Citation of manufacturer's or trade names does not constitute an official endorsement or approval of the use thereof.

Destroy this report when it is no longer needed. Do not return it to the originator.

Army Research Laboratory
Aberdeen Proving Ground, MD 21005-5069

ARL-TN-309 **April 2008**

Characterization of Solution Synthesis of Zinc Complexes With Iron

Amirh Whitt and James M. Sands
Weapons and Materials Research Directorate, ARL

REPORT DOCUMENTATION PAGE	Form Approved OMB No. 0704-0188

1. REPORT DATE *(DD-MM-YYYY)*	2. REPORT TYPE	3. DATES COVERED (From - To)
April 2008	Final	December 2003–December 2005

4. TITLE AND SUBTITLE
Characterization of Solution Synthesis of Zinc Complexes With Iron

5a. CONTRACT NUMBER

5b. GRANT NUMBER

5c. PROGRAM ELEMENT NUMBER

6. AUTHOR(S)
Amirh Whitt and James M. Sands

5d. PROJECT NUMBER
AH84-COMP02

5e. TASK NUMBER

5f. WORK UNIT NUMBER

7. PERFORMING ORGANIZATION NAME(S) AND ADDRESS(ES)
U.S. Army Research Laboratory
ATTN: AMSRD-ARL-WM-MD
Aberdeen Proving Ground, MD 21005-5069

8. PERFORMING ORGANIZATION REPORT NUMBER
ARL-TN-309

9. SPONSORING/MONITORING AGENCY NAME(S) AND ADDRESS(ES)

10. SPONSOR/MONITOR'S ACRONYM(S)

11. SPONSOR/MONITOR'S REPORT NUMBER(S)

12. DISTRIBUTION/AVAILABILITY STATEMENT
Approved for public release; distribution is unlimited.

13. SUPPLEMENTARY NOTES

14. ABSTRACT
The purpose of this report is to demonstrate the impact of process and materials variables on the characteristics of a Curie-limited susceptor based upon $Co_{(2-2x)}Zn_{2x}Ba_2Fe_{12}O_{22}$ formed using a solution-processing approach. $Zn_2Ba_2Fe_{12}O_{22}$ (Zn2Y) was the focus of this report, which has a Curie temperature of approximately 130 °C. The prepared particles were characterized using x-ray diffraction, environmental-scanning microscopy, x-ray photoelectron spectroscopy, and a vibrating sample magnetometer (VSM). Some basic observations and experimental results are provided for each method. VSM was determined to be among the most sensitive methods for characterization. Process variations produced significant product variations, but sources and causes were not fully isolated through this study. An ongoing effort to determine process controls for optimization and scale-up of particle processing of zinc-based compounds will be the focus of future works.

15. SUBJECT TERMS
Curie particles, zinc complex, solution synthesis, characterization, susceptor

16. SECURITY CLASSIFICATION OF:			17. LIMITATION OF ABSTRACT	18. NUMBER OF PAGES	19a. NAME OF RESPONSIBLE PERSON
a. REPORT	b. ABSTRACT	c. THIS PAGE			Amirh Whitt
UNCLASSIFIED	UNCLASSIFIED	UNCLASSIFIED	UL	22	19b. TELEPHONE NUMBER (*Include area code*) 410-306-0878

Standard Form 298 (Rev. 8/98)
Prescribed by ANSI Std. Z39.18

Contents

List of Figures

List of Tables

INTENTIONALLY LEFT BLANK.

1. Introduction

1.1 Joining Polymer Matrix Composite Materials

The use of polymer matrix composite materials and other materials has been implemented to lighten the forces of the U.S. Army. One challenge to using these materials is joining composite structures (*1, 2*). The standard ways of joining polymer matrix composites are by using mechanical fasteners and surface-bonding techniques. Incorporating mechanical fasteners into the composite structure usually creates weaknesses in the material. Because of this, surface bonding of the materials is preferred (*3*). One surface-bonding material that is commonly used is an elevated temperature-cure thermosetting adhesive. These thermosetting adhesives typically require temperatures of 120–200 °C for 5 to 120 min to completely cure (*4*). Existing techniques for heating the bondlines include using convection ovens, thermal blankets, and radiant heaters. Each of these processes heats the surface of the adherend, and the heat is conducted to the bondline. This presents a number of problems. The processing time is lengthened because of the time it takes to conduct the heat through the adherend. This reduces the efficiency of the process. Also, thermal losses from the structure and insulating composites cause surface temperatures to be significantly higher than bondline curing temperatures, and thus the control temperature may be near the degradation limits of the composite. Temperature sensors are often needed at the bondline to make sure it is heated uniformly and to the correct temperature. This presents additional complications to the field level repair procedures. The use of induction-heating methods would eliminate some traditional complications for field level adhesive repair in composite structures.

1.2 Induction Heating

Induction heating occurs when a susceptor material is exposed to a high-frequency electromagnetic field. A susceptor material is either an electrically conductive or magnetic material that heats up when exposed to an electromagnetic field. If the material is conductive, then eddy currents are induced by the electromagnetic field, and resistive effects generate heat. If the material is magnetic, then hysteresis heating occurs from losses in the magnetization-demagnetization cycles (*5*).

Using induction heating has advantages that conventional adhesive-curing techniques do not have. The adhesive can be cured without direct contact with the bondline. This eliminates the problem of lengthened process time and of possible degradation because the electromagnetic field can penetrate through the adherend, heating the bondline but not the adherend. This can be achieved by using a susceptor-doped adhesive. Using magnetic susceptors is more advantageous than conducting susceptors. This is because of the temperature control that the magnetic susceptor materials provide. Conducting-susceptor materials heat through the resistive effects of

eddy currents. The problem is that eddy currents keep producing heat energy as long as the susceptor material is exposed to the electromagnetic field and the susceptor does not decompose. Using these types of materials would require the addition of temperature feedback loops, embedded sensors, or another temperature regulation mechanism. Magnetic susceptor materials, however, possess a unique temperature regulation capability as a result of the Curie phenomenon (*6*). These susceptors have a Curie temperature, a temperature above which the material loses its magnetism. Once the magnetism is lost, the material is no longer affected by the electromagnetic field, and, therefore, the material cannot heat beyond this limit. Consequently, the susceptor is self-regulating. Magnetic susceptor materials can be fabricated with Curie temperatures that match a desired processing temperature for a given adhesive. Thus the susceptor imparts a self-regulated temperature limit to the adhesive when inserted into an electromagnetic field and eliminates the need for any temperature sensing and feedback.

The purpose of this experiment is to synthesize variants of the well-known Curie-limited susceptors based upon $Co_{(2-2x)}Zn_{2x}Ba_2Fe_{12}O_{22}$ using a solution-gelation–processing approach. In subsequent studies, the prepared particles will be blended with various adhesives to demonstrate the value of self-regulated curing for adhesive repair. $Zn_2Ba_2Fe_{12}O_{22}$ (Zn2Y) was the focus of this report and has a Curie temperature of ~130 °C.

2. Experimental

2.1 Synthesis

The procedure for synthesizing the Zn2Y susceptor is achieved using solution and gelation chemistry. Since iron hydroxide is hydroscopic and difficult to maintain in hydrated form (and extremely caustic), a reproducible concentration of $Fe3^+$ is established by dissolving $FeCl_3*6H_2O$ in distilled water. $Fe(OH)_3$ is precipitated from the solution by changing the pH to 14 with the addition of ammonium hydroxide.

$$Fe^{3+} + 3\ Cl^- + 3\ NH_4OH \rightarrow Fe(OH)_3 + 3\ NH_4^+ + 3\ Cl^- . \quad (1)$$

The solid $Fe(OH)_3$ was filtered from the basic solution via vacuum filtration. The still-wet $Fe(OH)_3$ was added to a previously established acidic solution of barium and zinc ions, created using ZnO and BaCO3, both of which are water-soluble.

$$Fe(OH)_3 + Zn^{2+} + Ba^{2+} \rightarrow Fe^{3+} + Zn^{2+} + Ba^{2+} + 3\ OH^- . \quad (2)$$

The ionic mixture is stirred on low heat for 30 min, and then further mixed at ambient temperature over night (6–12 hr). Ethylene glycol is then added to the ionic cocktail and lightly heated for 2–3 hr. The heat is then raised in order to evaporate the water and is continued until a

black tar remains in the beaker. The recovered product is then transferred into a ceramic tray and baked at 600 °C for 5 hr. The powder is then ground using a mortar with pestle before continuing the sintering process by heating at 1125 °C for 5 hr.

$$12\ Fe^{3+} + 2\ Zn^{2+} + 2\ Ba^{2+} + HEAT \rightarrow Zn_2Ba_2Fe_{12}O_{22}. \quad (3)$$

The completed synthesis is represented from starting materials as

$$12\ Fe(OH)_3 + 2\ ZnO + 2\ BaCO_3 \rightarrow Zn_2Ba_2Fe_{12}O_{22} + 2\ CO_2 + 18\ H_2O. \quad (4)$$

Table 1 is a summary of batch synthesis and variables changed in subsequent synthesis attempts. Sample identification (A–E) is established through this table to indicate variation in properties throughout this report.

Table 1. Summary of batch variations during synthesis of Zn2Y.

Sample	Variations on Standard Preparatory Method
A	Grinding in mortar with pestle after heating at 600 °C and 1125 °C.
B	Grinding in mortar with pestle after heating at 600 °C.
C	Grinding in mortar with pestle after heating at 1125 °C.
D	Grinding in mortar with pestle after heating at 1125 °C.
E	No grinding at all. Prepared using $BaCO_3$ dried in oven at 140 °C for 5 days.

Table 2 is a summary of the stoichometric measurements used in producing the various samples. Due to small measurement error, properties of some samples may be traceable to initial mixing conditions.

Table 2. Differences in initial measurements for Zn2Y samples.

Chemical	Theor.	A		B		C		D		E	
	Mass (g)	Mass (g)	Error (%)	Mass (g)	Error (%)	Mass (g)	Error (%)	Mass (g)	Error (%)	Mass (g)	Error (%)
$FeCl_3*6H_2O$	11.36	11.46	–0.87	11.97	–5.35	12.26	–7.91	12.11	–6.59	11.35	0.05
$BaCO_3$	1.38	1.35	2.34	1.40	–1.28	1.46	–5.62	1.38	0.17	1.38	–0.04
ZnO	0.57	0.57	0.02	0.58	–1.73	0.62	–8.75	0.61	–6.99	0.57	–0.05

2.2 Characterization

When characterizing the materials, four instruments were used. The Lake Shore Vibrating Sample Magnetometer Model 7300, the Siemens X-Ray Diffractometer D5005, the Hitachi S-4700 scanning electron microscope, and the ElectroScan Model 2020 environmental scanning electron microscope (ESEM).

2.2.1 Vibrating Sample Magnetometer

The vibrating sample magnetometer (VSM) measures the magnetization properties of materials and, hence, will measure the behavior of Zn2Y as an induction heating susceptor. To measure the magnetic properties of a given material, the VSM mechanically vibrates the material causing an alternating magnetic field. This magnetic field induces a current in coils on either side of the sample chamber. The VSM measures the induced current and uses it and the vibration frequency to calculate the magnetic properties of the material. The VSM characterized the magnetic response as a function of temperature. Ideally, Zn2Y maintains constant magnetization until the Curie temperature, 130 °C, where it instantaneously drops to zero magnetization. Experimental samples show a sharp reduction in magnetization around the Curie temperature. As shown in figure 1, all of the samples show behavior characteristic of Zn2Y-type materials. However, the optimization of these materials is desirable. Samples C, D (figures 2 and 3), and E behave closest to ideal. Samples A and B (figures 4 and 5) lose magnetization almost linearly. Samples C, D, and E were not ground in between baking at 600 °C and 1125 °C. This intermediate grinding may negatively affect the magnetic properties of the susceptor.

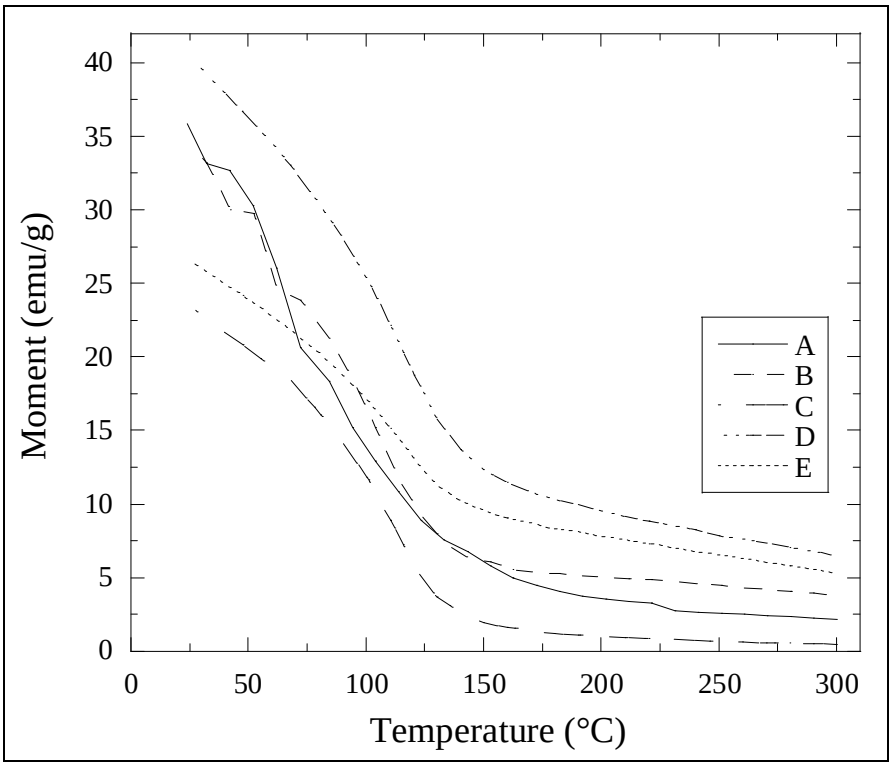

Figure 1. Magnetization curves for Zn2Y samples.

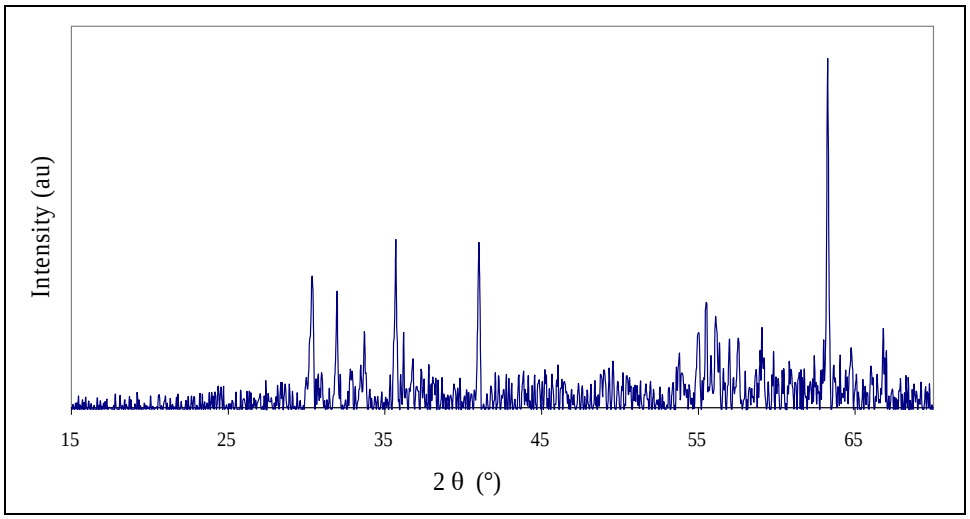

Figure 2. X-ray spectrum of sample C.

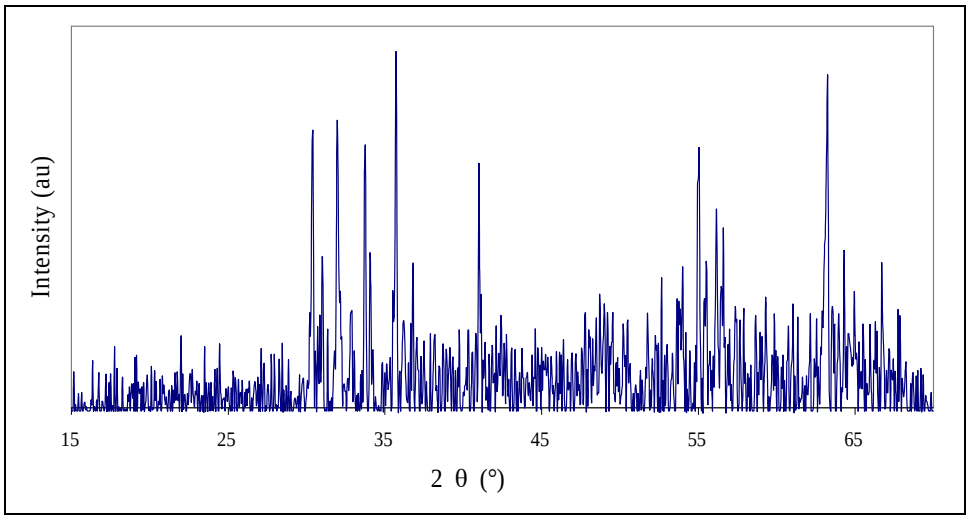

Figure 3. X-ray spectrum of sample D.

2.2.2 X-ray

X-ray diffraction uses x-rays to penetrate solid materials. The scattered incident radiation is collected as intensity as a function of scattering angle. Using Braggs Law, $\lambda = 2d \sin\theta$ where λ is the wavelength of the x-rays, *d* is the distance between the lattice planes in the material structure and θ is the angle of incidence of the x-rays, the experimental sample can be converted into a diffraction pattern representative of the crystal structure for Zn2Y. After the x-ray spectrum is obtained, it can be compared to those stored in a database of known materials and potentially matched according to its crystal structure. When characterizing Zn2Y, the x-ray diffraction was used as a time-efficient tool to quickly analyze the final product. The x-ray

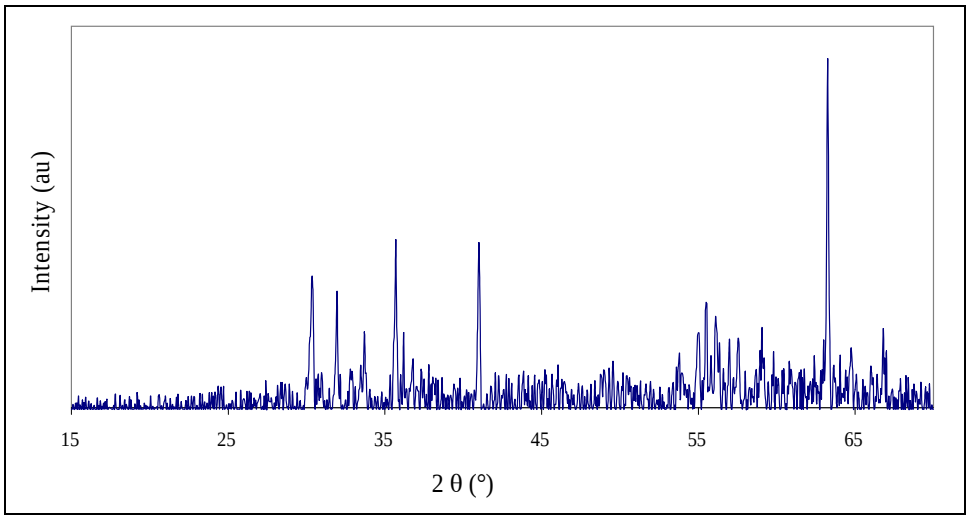

Figure 4. X-ray spectrum of sample A.

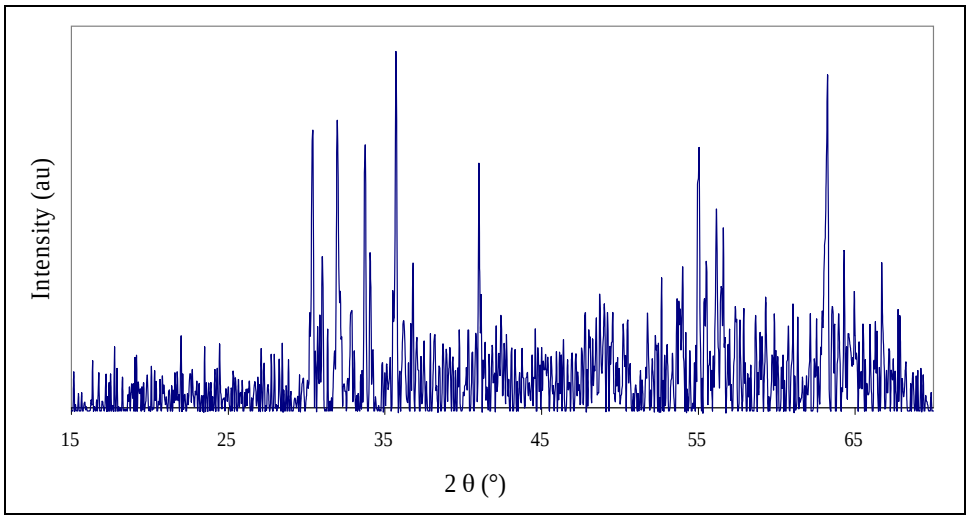

Figure 5. X-ray spectrum of sample B.

spectra produced for the Zn2Y samples are characteristic of the diffraction pattern for this type of material. The peak intensities vary slightly between the samples, but the peaks are all in the expected positions with the exception of one peak in the spectrum for sample A. There is a peak at $2\theta = 44.55°$ that is uncharacteristic of Zn2Y-type material. This peak matches the position and intensity of a silicon oxide, which could be the result of sample stage background not being subtracted.

2.2.3 Environmental Scanning Electron Microscope

An ESEM uses a highly focused beam of electrons to scan the sample. A key advantage to the ESEM is the effective conductivity afforded by the sample and the conductive water and helium

atmosphere. Consequently, even nonconductive materials can be investigated without the need for metallic coatings, allowing for precise evaluation of structural features at high magnifications. When the electron beam rasters across the sample, 2–10 keV electrons induce an electronic cascade of secondary electrons from the sample surface. These secondary electrons are collected at a detector to produce an image of the structures in the sample surface. The image is determined by the number of electrons emitted at each point on the sample. The ESEM images showed that Zn2Y is composed of platelets. It also shows that the platelets are on average >10 μm. This size is too large for practical inclusion into adhesive resins in the as-formed state, and, therefore, additional post-synthetic processing is necessary. The ESEM image for sample A is shown in figure 6. Additional images are shown in figures 7–9. Each image shows platelet-shaped particles that are clustered together.

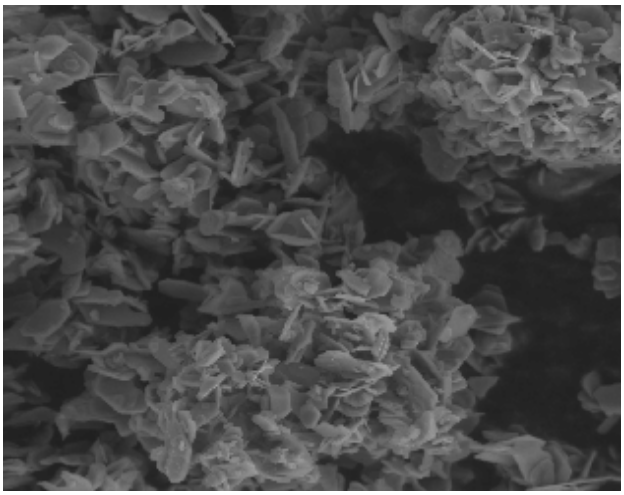

Figure 6. Image of sample A taken with electroscan model 2020 ESEM at 1000× magnification.

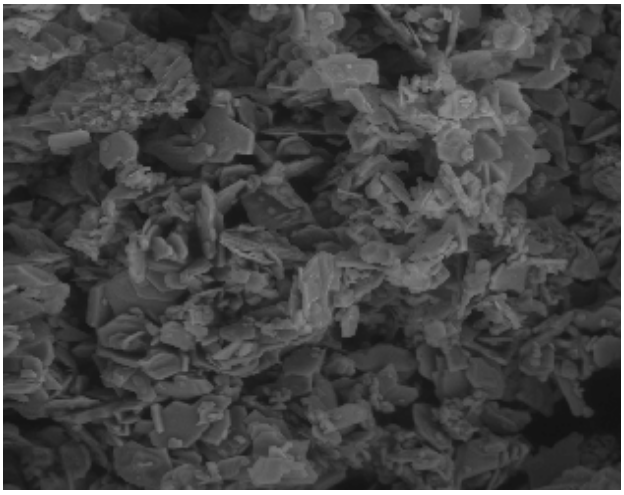

Figure 7. Image of sample B taken with electroscan model 2020 ESEM at 1000× magnification.

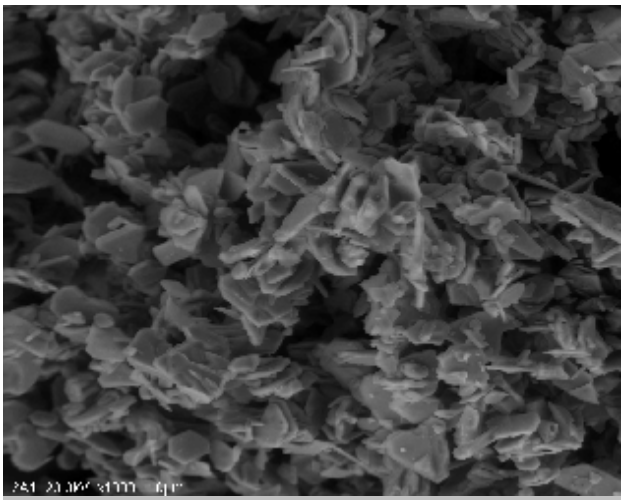

Figure 8. Image of sample C taken with electroscan model 2020 ESEM at 1000× magnification.

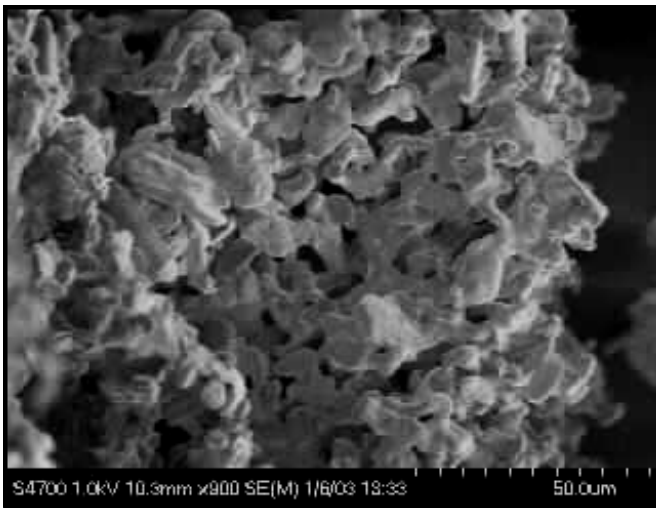

Figure 9. Image of sample E taken with Hitachi S-4700 ESEM at 900× magnification.

2.2.4 Energy Dispersive Auger X-ray Spectroscopy

Energy dispersive x-ray spectroscopy (EDS) is a chemical microanalysis technique performed in conjunction with an ESEM. The technique utilizes x-rays that are emitted from the sample during bombardment by the electron beam to characterize the elemental composition of the analyzed volume. When the electron beam of the ESEM bombards the sample, electrons are ejected from the atoms comprising the sample's surface. An electron from a higher shell fills a resulting electron vacancy, and an x-ray is emitted to balance the energy difference between the two electrons. The EDS x-ray detector measures the number of emitted x-rays vs. their energy.

The energy of the x-ray is characteristic of the element from which the x-ray was emitted. A spectrum of the energy vs. relative counts of the detected x-rays is obtained and evaluated for qualitative and quantitative determinations of the elements present in the sampled volume.

The resulting plots in figures 10–12 show that the ion concentrations of the elements in the samples are not as expected. This could be the result of poor initial mixing or loss of materials in the processing. Further, the uniformity of particle distribution may be of concern. Further investigation is required to understand these results. However, since the material shows such sensitivity to processing, the likelihood of continuing this project is low.

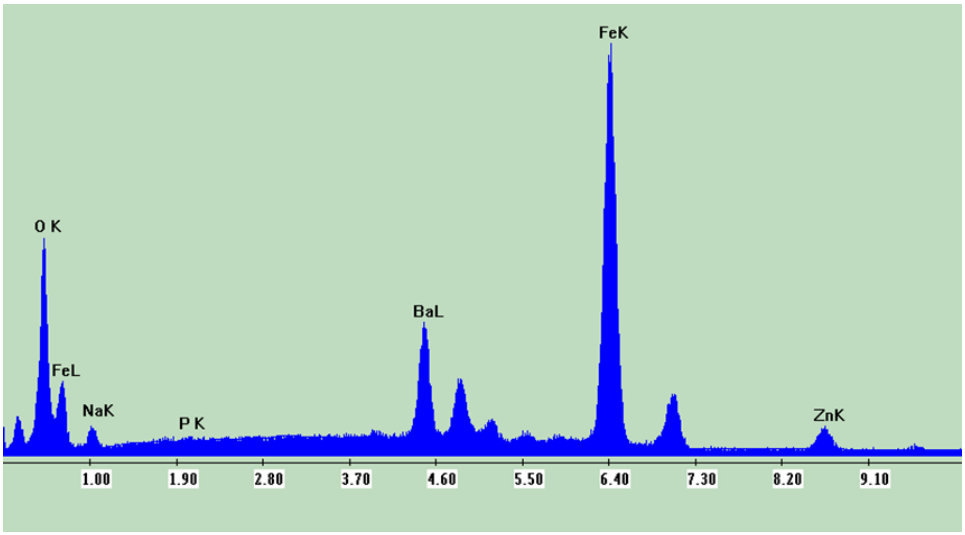

Figure 10. Elemental analysis of sample A taken with electroscan model 2020 ESEM.

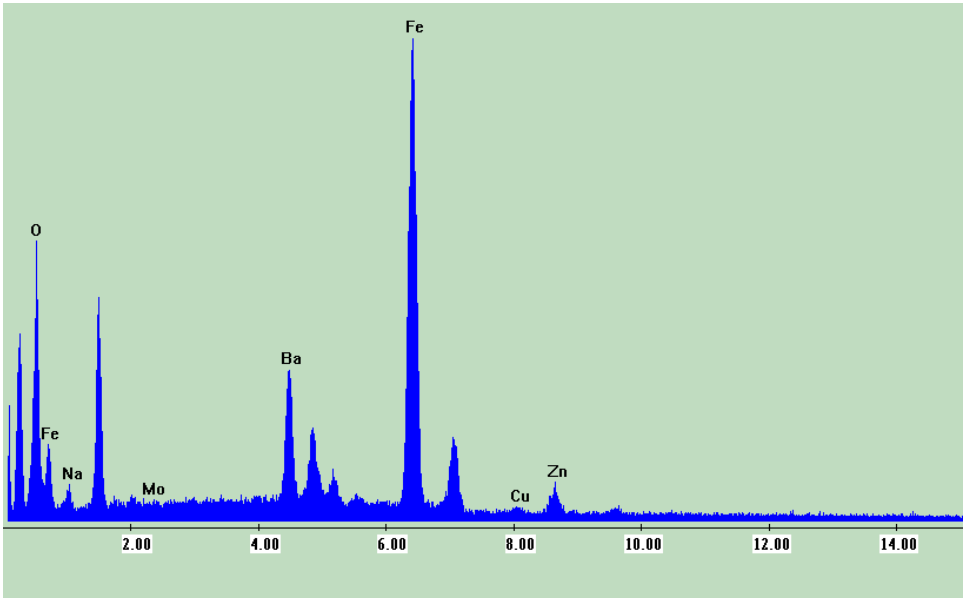

Figure 11. Elemental analysis of sample B taken with electroscan model 2020 ESEM.

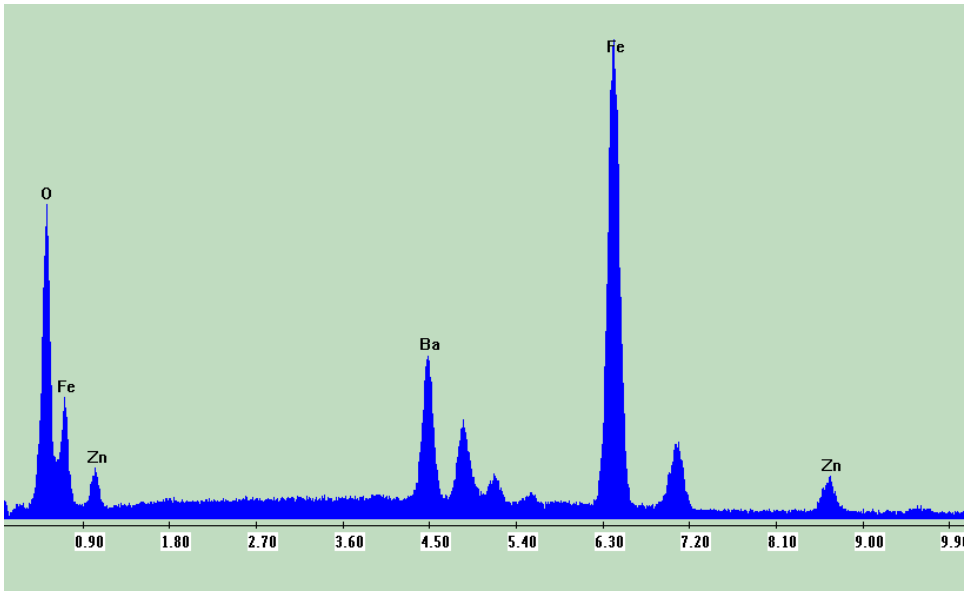

Figure 12. Elemental analysis of sample C taken with electroscan model 2020 ESEM.

An attempt was made to quantify the elemental compositions in the samples using the area function on the EDAX collector. The measured elemental concentrations of Ba, Zn, and Fe for sample A are shown in table 3. The measured molar concentration is based on raw materials weighed (table 1), and EDAX ∫ is the measurement based on peak area from the EDAX. The author does not know why Zn is so low in the EDAX, but this could be evidence of not achieving the Curie particles desired. Lack of Zn would also explain the poor magnetometer performance observed in figure 1.

Table 3. Ratios of ion concentrations for Ba and Zn compared to Fe (sample A not normalized).

Atomic Symbol	**Chemical Formula Weight (g)**	**Measured Mass (g)**	**Variation (%)**	**EDAX Integration (area)**	**Variation (%)**
Ba	0.17	0.24	–0.43	0.25	–0.48
Fe	1.00	1.00	0	1	0
Zn	0.17	0.32	–0.94	0.06	0.64

3. Conclusions

Using the materials analysis techniques discussed previously, major problems and solutions with the solution-gelation method for synthesizing Zn2Y have been identified. Material performance as an induction heating susceptor is affected by two major components—the elemental composition and the particle specifics of the material. The elemental composition can be affected by the precision of the composition measurements and the water content in the starting materials. The specifics of the material are the average size, shape (spherical vs. planar, etc.), and roughness. Also affecting the performance is the particle concentration when mixed into the media. ESEM data shows that eliminating the break in the final heating process significantly reduces the size of the particles. The EDAX data shows that something must be wrong with the starting materials because ion concentrations don't agree with each other. This was confirmed when the starting materials were tested using x-ray diffraction, and problems were found with most of the starting materials. The VSM data shows that the material doesn't perform ideally. But its magnetization vs. temperature curve is characteristic of the material. The x-ray spectrum shows that the ion concentrations are not correct because the peak intensities don't match with the intensity pattern of Zn2Y-type material.

4. References

1. Hahn, G. L.; Bergstrom, L. K.; Border, J. N.; McIlroy, B. E. *Induction Heating Repair of Structures*; final report F33657-88-C-0087; McDonnell Douglas Corporation: St. Louis, MO, October 1991.

2. Tay, T. E.; Fink, B. K.; McKnight, S. H.; Yarlagadda, S.; Gillespie, J. W., Jr. Accelerated Curing of Adhesives in Bonded Joints by Induction Heating. *J. Comp. Mater.* **1999**, *33* (17), 1643–1664.

3. Consenza, F. Mechanical Fasteners for Composites. *Materials Engineering* **1987**, *104* (8), 33–37.

4. Marinelli, J. M.; Lambing, C. L. T. Study of Surface Treatments for Adhesive Bonding of Composite Materials. *Advanced Materials: Performance Through Technology Insertion International SAMPE Symposium and Exhibition Proceedings*, Anaheim, CA, 10–13 May 1993; SAMPE: Covina, CA, 1993; Vol. 38, pp 1196–1210.

5. Yungwirth, C. J.; Wetzel, E. D.; Sands, J. M. *Induction Curing of Phase Toughening Adhesive*; ARL-TR-2999; U.S. Army Research Laboratory: Aberdeen Proving Ground, MD, February 2003.

6. Sadiku, M. N. O. *Elements of Electromagnetics*, 2nd ed.; Oxford University Press: New York, 2001.

NO. OF COPIES	ORGANIZATION
1 (PDF ONLY)	DEFENSE TECHNICAL INFORMATION CTR DTIC OCA 8725 JOHN J KINGMAN RD STE 0944 FORT BELVOIR VA 22060-6218
1	US ARMY RSRCH DEV & ENGRG CMD SYSTEMS OF SYSTEMS INTEGRATION AMSRD SS T 6000 6TH ST STE 100 FORT BELVOIR VA 22060-5608
1	DIRECTOR US ARMY RESEARCH LAB IMNE ALC IMS 2800 POWDER MILL RD ADELPHI MD 20783-1197
1	DIRECTOR US ARMY RESEARCH LAB AMSRD ARL CI OK TL 2800 POWDER MILL RD ADELPHI MD 20783-1197
1	DIRECTOR US ARMY RESEARCH LAB AMSRD ARL CI OK T 2800 POWDER MILL RD ADELPHI MD 20783-1197

ABERDEEN PROVING GROUND

1	DIR USARL AMSRD ARL CI OK TP (BLDG 4600)

INTENTIONALLY LEFT BLANK.